Accepted Article

Solanum tuberosum StCDPK1 is regulated by miR390 at the posttranscriptional level and phosphorylates the auxin efflux carrier StPIN4 in vitro, a potential downstream target in potato development

Franco Santin[a], Sneha Bhogale[b], Elisa Fantino[a], Carolina Grandellis[a,†], Anjan K. Banerjee[b,*] and Rita M. Ulloa[a,*]

[a]Instituto de Investigaciones en Ingeniería Genética y Biología Molecular, CONICET and Facultad de Ciencias Exactas y Naturales, Universidad de Buenos Aires. Vuelta de Obligado 2490 2[do] piso, 1428, Buenos Aires, Argentina

[b]Indian Institute of Science Education and Research, Biology Division, Dr. Homi Bhabha Road, Pune 411008, Maharashtra, India

*****Corresponding authors, e-mail: rulloa@dna.uba.ar; akb@iiserpune.ac.in

[†]Present address: Instituto de Biología Molecular y Celular de Rosario (IBR) Ocampo y Esmeralda, Predio CONICET-Rosario2000 Rosario, Santa Fe, Argentina

This article has been accepted for publication and undergone full peer review but has not been through the copyediting, typesetting, pagination and proofreading process, which may lead to differences between this version and the Version of Record. Please cite this article as doi: 10.1002/ppl.12517

This article is protected by copyright. All rights reserved.

Accepted Article

Among the many factors that regulate potato tuberization, calcium and Calcium Dependent Protein Kinases (CDPKs) play an important role. CDPK activity increases at the onset of tuber formation with StCDPK1 expression being strongly induced in swollen stolons. However, not much is known about the transcriptional and posttranscriptional regulation of StCDPK1 or its downstream targets in potato development. To elucidate further, we analyzed its expression in different tissues and stages of the life cycle. Histochemical analysis of StCDPK1::GUS plants demonstrated that StCDPK1 is strongly associated with the vascular system in stems, roots, during stolon to tuber transition, and in tuber sprouts. In agreement with the observed GUS profile, we found specific cis-acting elements in StCDPK1 promoter. In silico analysis predicted miR390 to be a putative posttranscriptional regulator of StCDPK1. qRT-PCR analysis showed ubiquitous expression of StCDPK1 in different tissues which correlated well with Western blot data except in leaves. On the contrary, miR390 expression exhibited an inverse pattern in leaves and tuber eyes suggesting a possible regulation of StCDPK1 by miR390. This was further confirmed by Agrobacterium co-infiltration assays. In addition, in vitro assays showed that recombinant StCDPK1-6xHis was able to phosphorylate the hydrophilic loop of the auxin efflux carrier StPIN4. Altogether, these results indicate that StCDPK1 expression is varied in tissue specific manner having significant expression in vasculature and in tuber eyes; is regulated by miR390 at posttranscriptional level and suggest that StPIN4 could be one of its downstream targets revealing the overall role of this kinase in potato development.

Introduction

Potato (*Solanum tuberosum*) is the most important non-grain crop (http://faostat.fao.org/). In its natural habitat, tubers serve as vegetative propagation organs that undergo a period of dormancy during cold winters and then sprout in the next spring to generate a new plant. *S. tuberosum* is divided into two slightly different subspecies: ssp. *andigena*, in which tuberization is under strict photoperiodic control and plants tuberize only under short day conditions (Rodriguez-Falcon et al. 2006) and ssp. *tuberosum*, the potato now cultivated around the world which was selected for long day tuberization (Kloosterman et al. 2013).

The process of tuber formation has been the focus of many research groups with the aim of improving yields and providing a model system to understand development of modified organs in plants. Tuberization is a complex developmental process that comprises inhibition of longitudinal growth of an underground stem, the stolon, followed by initiation and growth of a tuber (Cutter 1978). There is a switch in phloem unloading of assimilates in the subapical region of developing stolons, which subsequently become the largest sinks (Viola et al. 2001). In vitro, tuberization is induced by high sucrose concentration

This article is protected by copyright. All rights reserved.

Accepted Article

in the media (Xu et al. 1998). Both internal and external cues regulate tuberization; in particular it has been established that low levels of gibberellins (GAs) are essential to trigger tuber formation while environmental signals that promote tuber development affect GAs concentration in early stages of stolon development (Ulloa et al. 2012). Tuber formation requires changes in meristem identity and the reorientation of the plane of cell division (Xu et al. 1998). Although the underlying mechanism is still not completely understood and there is controversy in the field, it is generally accepted that reorientation and changes in cell division pattern in plants are mediated by auxin (Baskin 2015, Chen et al. 2014, Chen et al. 2016). During early tuber developmental stages, genes involved in auxin transport (*PIN* gene family), auxin response factors (*ARF*), and *Aux/IAA* genes are differentially expressed (Kloosterman et al. 2008) and auxin content increased in the stolons prior to tuberization (Roumeliotis et al. 2012a). Thus, it was postulated that the initiation and induction of potato tubers could be regulated by a crosstalk between GA and auxin (Roumeliotis et al. 2012b).

In plants, calcium (Ca^{2+}) is a key second messenger in many developmental processes. Experiments with calcium chelators and calmodulin antagonists suggested that both calcium and calmodulin are required in the early stages of potato tuberization (Balamani et al. 1986, Raices et al. 2003a). Calcium-dependent protein kinases, CDPKs, are unique calcium sensor/transducers that couple changes in Ca^{2+} levels to specific responses in metabolism, osmosis, hormone and stress signaling pathways (Boudsocq and Sheen 2013). CDPKs are present in protists, oomycetes, green algae and plants, but have not been identified in any animal or fungal genome (Valmonte et al. 2014). These enzymes are encoded by multigene families, whose members share a unique structure consisting of an N-terminal variable domain (NTV), a serine/threonine kinase catalytic domain fused through a junction region or autoinhibitory domain to a carboxyterminal calmodulin-like domain (CLD) with four EF hands Ca^{2+} binding sites (Harper et al. 1991). Expression and functional studies suggest the importance of CDPK gene expansion and diversification in different plant species during evolution. Enhanced CDPK activity/expression has been associated with developmental functions and with biotic and abiotic stress responses (Valmonte et al. 2014).

In potato, CDPK activity is enhanced at the onset of tuber development (MacIntosh et al. 1996) and its activity is found to be higher in the particulate fraction of swelling stolons (Raices et al. 2003a). Three potato CDPK isoforms, *StCDPK1*, 2 and 3, are expressed in tuberizing stolons; in particular *StCDPK1* is strongly induced in swollen stolons and its expression is enhanced by high sucrose in the medium (Raices et al. 2003b, Raices et al. 2003c). *StCDPK1, 2* and *3* belong to subgroup IIa and share the same gene structure (eight exons/seven introns). Despite the high homology in their kinase domains (Appendix S1), these three CDPK isoforms differ in their NTV domains, in their kinetic parameters (Km and Vmax) and also in their expression patterns (Gargantini et al. 2009, Giammaria et al. 2011, Grandellis et al. 2012),

This article is protected by copyright. All rights reserved.

Accepted Article

suggesting that each one plays a specific role. Potato plants with reduced expression of *StCDPK1* in stolons developed more tubers than wild type plants in the presence of hormones such as, abscisic acid, and 6-benzylaminopurine (ABA and BAP) that promote tuberization in potato. It was also observed that they were less sensitive to GA action (stolons were significantly shorter than those of control plants) suggesting that this kinase could be a converging point for the inhibitory and promoting signals that influence the onset of potato tuberization (Gargantini et al. 2009). At the protein level, StCDPK1 activity is regulated by calcium and autophosphorylation and this isoform has myristoylation and palmitoylation consensus in its NTV domain that are involved in targeting StCDPK1 to the plasma membrane (Gargantini et al. 2009, Grandellis et al. 2012, Raices et al. 2001, Raices et al. 2003c).

The transcriptional and posttranscriptional regulation of *StCDPK1* and its downstream targets in potato development has not been investigated. MicroRNAs (miRNAs) are important posttranscriptional regulators that function in many plant developmental and stress related pathways. miRNAs are small, endogenous, single-stranded and ~21–24 nt long RNAs that regulate gene expression by inducing degradation or repressing translation of targeted mRNAs (Zhang et al. 2013). Role of miRNAs in regulation of tuberization has also been reported, wherein *miR156* (Bhogale et al. 2014) and *miR172* (Martin et al. 2009) have been shown to play important roles. Our in silico studies predicted *StCDPK1* to be targeted by miR390 in potato. The present study is therefore an attempt to understand the transcriptional and posttranscriptional regulation of *StCDPK1* and to identify the potential targets of this kinase during potato development. A detailed study was undertaken to analyze *StCDPK1* transcription pattern in different tissues and stages of the potato vegetative life cycle using both qRT-PCR and characterizing CDPK1pro::GUS potato plants. In addition, we showed that, StCDPK1 is able to phosphorylate the hydrophilic loop of the potato auxin transporter StPIN4 in vitro, and addressed the putative *miR390*-mediated control of *StCDPK1* in potato development.

Materials and methods

Plant material

In this study, *S. tuberosum* cv Desirée wild-type plants and CDPK1pro::GUS plants were used. In vitro plants were micropropagated on a modified MS medium (Murashige and Skoog 1962) with the addition of 2% (w/v) sucrose and 0.7% (w/v) agar and maintained in a long day photoperiod (16/8 h light/dark) at 23°C. Alternatively, single node cuttings from CDPK1pro::GUS plants were grown under in vitro tuberization conditions: MS medium, 8% (w/v) sucrose and 0.7% (w/v) agar under complete darkness at 20°C during the indicated periods. Two-month-old soil grown plants were used for quantification experiments of *StCDPK1* and *miR390*. *Nicotiana benthamiana* plants were used for *Agrobacterium*-co-

This article is protected by copyright. All rights reserved.

Accepted Article

infiltration experiments. Soil grown plants were maintained in the greenhouse; natural light was supplemented 16 h per day by sodium lamps providing 100–300 μmol s^{-1} m^{-2}; the temperature was set at 26°C during day and 19°C in the night.

Isolation and sequence analysis of the StCDPK1 promoter region

The Genome Walker Universal kit (Clontech Labs Inc., Palo Alto, CA) was used to isolate the promoter sequence of *StCDPK1* gene (GenBank accession: DQ507862) according to the manufacturer's instructions. The gene specific primers were designed on the 5´UTR of StCDPK1, and named GSP1 for initial round of PCR reaction and GSP2 for nested PCR. All primer sequences used in this manuscript are listed in Appendix S2A. The final PCR product was cloned into pGEM®-T Easy (Promega, Madison, WI) via the TA cloning method and the construct was confirmed by sequencing at the DNA Facility at Iowa State University. Coinciding alignments of the 5'UTR of StCDPK1 and the obtained sequence confirmed the isolation of the promoter region. In silico analysis of *cis*-acting responsive elements was performed using PLACE (http://www.dna.affrc.go.jp/PLACE) (Higo et al. 1999) and PlantCare (http://bioinformatics.psb.ugent.be/webtools/plantcare/html/) (Lescot et al. 2002) databases and *P*-values were computed using FIMO tool from MEME Suite (Grant et al. 2011). The promoter was amplified with primers St1-prom-Fw and St1-prom-Rev (Appendix S2A) using Platinum® Taq DNA Polymerase High Fidelity (Invitrogen, Carlsbad, CA) and subcloned into the *Sal*I/*Xma*I sites of the pBI101 binary vector (Clontech Labs Inc., Palo Alto, CA) containing the β-glucuronidase (GUS) reporter gene (Appendix S3A). The construct was confirmed by sequencing at Macrogen Sequencing facility (Seoul, South Korea), and used to electro-transform *Agrobacterium tumefaciens* LBA4404 strain.

Transformation and plant regeneration

Excised leaves from 4-weeks-old in vitro potato plants were selected and used for *Agrobacterium* mediated transformations as described in (Grandellis et al. 2012). The fourteen independent CDPK1pro::GUS lines (A–N) obtained were confirmed by PCR using St1-470 and GUS-rev primers (Appendix S2A) and by fluorometric analysis of GUS activity (see Appendix S3B and C). Plants transformed with pBI101 binary vector containing the GUS gene (Clontech Labs Inc., Palo Alto, CA) but without the promoter sequence (empty vector) were used as negative controls (Appendix S3D).

Histochemical and fluorometric analysis

Expression of the GUS reporter gene was evaluated by incubating the tissue samples from soil or in vitro grown plants for 16 to 18 h at 37°C in GUS buffer containing 0.1 *M* $NaHPO_4$, pH 7.0, 1 m*M* X-GLUC (5-bromo-4-chloro-3-indolyl-*β*-D-GlcUA), 10 m*M* EDTA, 0.5 m*M* Potassium ferricyanide, 0.5 m*M* Potassium ferrocyanide and 0.1% Triton X-100. Samples were cleared with 70% ethanol several times and

This article is protected by copyright. All rights reserved.

Accepted Article

photographed employing a Leica EZ4D magnifying glass. For histology, stained samples were cut into 0.5–1 cm long pieces and embedded in 4% agarose or in Tissue-Tek O.C.T. compound (Sakura Finetek Inc., Torrance, CA). 10 µm or 30 µm sections were obtained using a Leica vibratome VT1200 or a Leica cryostat CM1850 (Leica Microsystems GmbH, Wetzlar, Germany). Sections were imaged using Leica microscope S8AP0.

In vitro tissue culture plants were homogenized using 500 µl of extraction buffer containing 100 m*M* sodium phosphate buffer, pH 7.0, 10 m*M* EDTA, 0.1% N-lauryl-sarcosine, 0.1% Triton X-100, 10 m*M* β-mercaptoethanol. Samples were then centrifuged at 13 000 *g* for 30 min, at 4°C. The supernatant was recovered and protein quantification was performed by Bradford. Protein extracts (10 µg) were incubated for 0, 15, 30, 45 min and 1 h at 37°C in 500 µl of extraction buffer containing 2.0 m*M* 4-methylumbelliferyl-beta-D-glucuronide (MUG). The reaction was stopped by transferring 20 µl aliquots to 1.98 ml of stop solution (0.2 *M* Na_2CO_3). The relative fluorescence was measured using a fluorometer Hoefer DyNAQuant 200 (Amersham Biosciences, San Francisco, CA) with an excitation wavelength of 365 nm and an emission wavelength at 460 nm. The specific activity of GUS was calculated using a calibration curve for 4-methylumbelliferone (4-MU).

Prediction of microRNAs targeting StCDPK1

MicroRNAs targeting StCDPK1 were predicted using psRNATarget online tool (plantgrn.noble.org/psRNATarget/) (Dai and Zhao 2011). Default parameters were used and sequences showing a score of 1 to 5 were considered. The psRNATarget results were further tested with another software, TargetAlign (http://www.leonxie.com/targetAlign) (Xie and Zhang 2010) using default parameters. Use of two softwares reduces the chances of false positive results.

Validation of *miR390*

miR390 precursor (GenBank Accession number CK247568.1) was amplified from total RNA harvested from in vitro potato plants. cDNA was prepared using oligo-dT primer followed by a PCR with *miR390* specific forward primer *miR390*preFP and reverse primer *miR390*preRP (Appendix S2A). The amplicon (835 bp) was confirmed by sequencing. Mature *miR390* was detected by stem-loop RT-PCR as described earlier (Varkonyi-Gasic et al. 2007). Total RNA was isolated by TRIzol reagent (Invitrogen, Carlsbad, CA) as per manufacturer's instructions and then treated with RQ1 RNase-Free DNase (Promega, Madison, WI). Reverse transcription was carried out using stem-loop primer *miR390*STP (Appendix S2A). The stem-loop reverse transcription primers provide better specificity and sensitivity than linear primers because of base stacking and spatial constraint of the stem-loop structure (Chen et al. 2005). End-point PCR was performed using *miR390*FP and universal reverse primer univRP (Appendix S2A) rendering a 61-bp amplicon that was cloned in pGEM-T Easy (Promega, Madison, WI) and was verified by

This article is protected by copyright. All rights reserved.

Accepted Article

sequencing.

Analysis of CDPK1 and *miR390* levels

CDPK1 and *miR390* transcript levels were determined by qRT-PCR. RNA was extracted from leaves, stems, roots, stolons, swollen stolons, tubers and tuber eyes (dormant) from two-month old soil grown Desirée wild-type plants by TRIzol (Invitrogen, Carlsbad, CA) as per manufacturer's instructions. One µg total RNA was used for cDNA synthesis using oligodT primer for CDPK1 and stem-loop reverse primer for *miR390* (STP). All qPCR reactions were performed on Mastercycler Eppendorf Realplex using KAPA SYBR green master mixture (Kapa Biosystems, Wilmington, MA). For CDPK1 expression analysis, CDPK1 FP and CDPK1 RP primers (Appendix S2A) were used. The reactions were carried out at 95°C for 2 min followed by 40 cycles of 95°C for 15 s; 56°C for 15 s and 72°C for 20 s. GAPDH was used for normalization using GAPDH FP and GAPDH RP primers (Appendix S2A) with PCR conditions same as for CDPK1. Levels of *miR390* were determined by stem-loop qRT-PCR method. Reverse transcription was carried out using stem-loop reverse primer *miR390*STP as per the protocol (Varkonyi-Gasic et al. 2007), and qPCR was performed using *miR390*FP and univRP primers (Appendix S2A). qPCR reactions were performed at 95°C for 5 min followed by 40 cycles of 95°C for 5 s, 60°C for 10 s and 68°C for 8 s. PCR specificity was checked by melting curve analysis (Appendix S2B). The relative mRNA levels were presented as $2^{(\text{Ct/housekeeping gene-Ct/gene of interest})}$ as reported in (Yang et al. 2013). Additionally, proteins from the plant tissues were extracted with buffer A (50 m*M* Tris-HCl, pH 6.8, 1% β-mercaptoethanol, and 0.2% PVP) as described in Giammaria et al. (2011). Aliquots (50 µg) were subjected to SDS-PAGE and Western blot analysis.

Generation of 35S::StCDPK1-6xHis, 35S::StCDPK7-6xHis and35S::*miR390*pre constructs

StCDPK1 (GenBank accession number AF115406) and StCDPK7 (GenBank accession number KJ830932) coding sequences and *miR390* precursor sequence were amplified from potato whole plant tissue using forward primers St1FP, St7FP or *miR390*preFP and reverse primers St1RP, St7RP or *miR390*preRP (Appendix S2A). Amplicons were subcloned into the BamHI/XhoI sites of pENTR2B and subsequently cloned, using GATEWAY technology, into pGWB408 vector in frame with a C-terminal 6xHis tag. The resulting constructs were under the control of 35S promoter. The 35S::CDPK-6xHis and 35S::*miR390*pre clones were sequenced in Macrogen sequencing facility and used for *Agrobacterium*-mediated co-infiltration experiments.

***Agrobacterium* co-infiltrations**

Agrobacterium-co-infiltrations were performed in *N. benthamiana* leaves (6 week old plants) using *A. tumefaciens* GV3101 or AGL1 strains transformed with 35S::*miR390*precursor, 35S::CDPK1-6xHis,

This article is protected by copyright. All rights reserved.

Accepted Article

35S::CDPK7-6xHis, or pGWB408 (empty vector). After overnight culture, bacteria were precipitated, resuspended in 10 m*M* $MgCl_2$, 10 m*M* MES-K: pH5.6, 100 µ*M* acetosyringone, adjusting the absorbance (OD_{600nm}) to 0.4, and left at room temperature for 2 h prior infiltration. To co-express more than one construct, the corresponding cultures were mixed and incubated at room temperature for 2 h and co-injections were performed. Leaves were infiltrated with buffer (control), empty vector (EV), EV plus 35S::CDPK1 (CDPK1), EV plus 35S::*miR390*precursor (*miR390*) or EV plus 35S::CDPK7 (CDPK7). In addition, co-agroinfiltrations were performed simultaneously with EV, CDPK1 and *miR390* (CDPK1/*miR390*) or with EV, CDPK7 and *miR390* (CDPK7/*miR390*). At least six leaves from independent plants were agroinfiltrated for each condition. Leaves were harvested 3 days post infiltration for further analysis at the transcript or protein level. The qRT-PCR reactions were performed as described previously and data was analyzed using $2^{-\Delta\Delta Ct}$ method (Livak and Schmittgen 2001). For CDPK7 expression, CDPK7 FP and RP primers were used (Appendix S2A). Proteins from agroinfiltrated *N. benthamiana* leaves were extracted with buffer A (50 m*M* Tris-HCl, pH 6.8, 1% β-mercaptoethanol, and 0.2% PVP) as described in Giammaria et al. (2011) and aliquots (50 µg) were subjected to 10% SDS-PAGE and Western blot assays.

Western blot assay

SDS–PAGE of protein samples were performed using a Bio□Rad Mini-Protean Tetra Cell apparatus (Bio-Rad Laboratories Inc., Hercules, CA) as per the manufacturer's instructions. Subsequently, proteins were transferred onto an Amersham Hybond-ECL nitrocellulose membrane (GE Healthcare Life Sciences, Marlborough, MA). CDPK1 detection in protein extracts from the different tissues was performed using an anti-CDPK1 antibody (dilution 1:300) (Gargantini et al. 2009) and a HRP-conjugated anti-rabbit IgG secondary antibody (sc-2004, dilution 1:5000). Protein extracts from co-agroinfiltration assays were analyzed with the HRP-conjugated anti-polyhistidine antibody (sc-8036) that recognizes the C-terminal 6xHis tag present in StCDPK1 or StCDPK7 fusion proteins. Protein loading was assessed using a commercial anti-α tubulin antibody (TU-02, 1:5000) and a HRP-conjugated anti-mouse IgG secondary antibody (sc-2005, 1:5000) . Western blot analysis of StCDPK1 and StCDPK7 recombinant proteins was performed with the anti-CDPK1 antibody followed by the HRP-conjugated anti-rabbit IgG secondary antibody or with the HRP-conjugated anti-polyhistidine antibody (Appendix S4A). TU-02, sc2004, sc-2005 and sc-8036 antibodies were from Santa Cruz Biotechnology Inc., Dallas, TX. Blots were developed with ECL reagent (Amersham Pharmacia Biotech, Amersham, UK) according to the manufacturer's instructions**.** The chemiluminescence was detected using GeneGnome XRQ (Syngene, Cambridge, UK).

Generation of recombinant proteins

The nucleotide sequence (793 bp) encoding the hydrophilic loop of the auxin transporter StPIN4

This article is protected by copyright. All rights reserved.

Accepted Article

(PGSC0003DMT400078330) was amplified using primers StPINFP and StPINRP (Appendix S2A). The amplicon was subcloned into the *Nco*I and *Not*I restriction sites of the expression vector pET28a(+) in frame with a C-terminal 6xHis tag. The construct was confirmed by sequencing and subsequently transformed into *E. coli* BL21 Shuffle strain. Additionally, *E. coli* cells were transformed with plasmid pET15b(+) encoding the tobacco phenylalanine ammonia lyase isoform 3 tagged with 6xHis (NtPAL3-6xHis, 80 kDa) that was kindly provided by Dr. Richard A. Dixon (Reichert et al. 2009) or with plasmid pET22b(+) encoding 6xHis-tagged StCDPK1 (Grandellis et al. 2012). Bacterial cultures were induced with 1 m*M* IPTG at 30°C during 4 h. After sonication (6 cycles, 10 s each) at 4°C, the lysates were centrifuged at 20 000 *g* during 30 min and the supernatants were purified by affinity chromatography using nickel agarose columns Ni-NTA agarose (QIAGEN GmbH, Hilden, Germany) as per the manufacturer's instructions. Western blot analysis was performed to confirm the presence of the StPIN4HL-6xHis protein (30kDa, Appendix S4B).

Phosphorylation assays

Aliquots of StPIN4HL-6xHis or NtPAL3-6xHis recombinant proteins were incubated during 5 min at 30°C with StCDPK1-6xHis (0.1 µg) in the presence of 1 m*M* EGTA or 25 µ*M* calcium. The reaction mixture contained 20 m*M* Tris-HCl, pH 7.5, 10 m*M* $MgCl_2$, 10 m*M* β-mercaptoethanol and 10 µ*M* [γ-^{32}P]-ATP (specific activity 500 cpm pmol^{-1}) in a final volume of 40 µl. Autophosphorylation of StCDPK1 was performed in the same conditions. Two series of reactions were performed in parallel. Reactions were stopped with the addition of cracking buffer and boiled for 3 min. After 10 or 12% SDS-PAGE, one gel was transferred to nitrocellulose membranes and exposed to Amersham Hyperfilm (GE Healthcare Ltd., Buckinghamshire, UK), and the other one was stained with Coomassie Brilliant Blue to assess protein loading.

2D gel electrophoresis assays

StCDPK1-6xHis (100 µg) was subjected to an autophosphorylation assay in the presence of 25 µ*M* calcium and was then analyzed by 2D gel electrophoresis as described in Grandellis et al. (2012) using strips ranging from pH 4 to 7 and 10% acrylamide gels. The gel was transferred to nitrocellulose and analyzed by Western blot.

Statistical analysis of qRT-PCRs

Plant tissue expression data were analyzed with GraphPad Prism 6.07 using two-way ANOVA (analysis of variance) followed by Tukey's multiple comparison test (P<0.05) while one-way ANOVA followed by Tukey's multiple comparison test (P<0.05) was used in agroinfiltration experiments.

This article is protected by copyright. All rights reserved.

Accepted Article

Results

Isolation and in silico analysis of *StCDPK1* promoter sequence

A 2273-bp sequence upstream from *StCDPK1* start codon was cloned using the Genome Walker kit and sequenced. Plant promoters typically contain proximal and distal regulatory elements within a range from 1 to 2 kb upstream from their transcription start site (Dutt et al. 2014, Liu and Stewart 2016). Therefore, the cloned sequence was presumed to include the majority of the elements controlling gene expression. When the *S phureja* genome (http://potato.plantbiology.msu.edu/cgi-bin/gbrowse/potato/) (Potato Genome Sequencing et al. 2011) was released, this sequence together with the complete genomic sequence of *StCDPK1* was blasted (blastn) against PGSC *S. tuberosum* group Phureja DM1-3superscaffold (v3) database. The best hit was PGSC0003DMB000000589 (98.05% identity, score 5352 bits, E value 0.0), which was located at chromosome 12, position 9046 kbp confirming our previous data (Gargantini et al. 2009). The 100 kb region surrounding *StCDPK1* (PGSC0003DMG400027877) contains only five genes (Appendix S5A); the nearest upstream gene encoding a RING-H2 finger protein is 20.4 kb apart, while the nearest downstream gene, encoding an ubiquitin protein ligase is 26.2 kb apart.

In silico analysis of the *cis*-acting elements present in *StCDPK1* promoter retrieved 12 motif occurrences with a *P*-value <0.0001 (Table 1). According to PLACE and PlantCare databases, these elements regulate root-specific and storage protein genes or confer light-, gibberellin- or ABA-responsiveness. It is noteworthy the presence of AC-I and AC-II elements (Table 1) that enhance expression of genes in xylem (Hatton et al. 1995, Hauffe et al. 1993). The AC-I and AC-II elements identified by PlantCare database (matrix score of 9 and 8.5 respectively) are in the same position (990 bp upstream of the ATG codon in the + strand). When using the unifying matrix for AC element identification [C(C/T)CACC(T/A)ACC] as reported in (Raes et al. 2003), one element with 2 mismatches (CATACCTACC) was identified. Additionally, other root specific (P<0.01), cytokinin-responsive (P<0.001), and osmotic-, drought- and salinity-responsive elements (P<0.001) were abundant in StCDPK1 promoter, (Appendix S5B).

StCDPK1 expression analysis

According to DM and RH RNA-Seq data available at the potato genome browser (potato.plantbiology.msu.edu/cgi-bin/gbrowse/), *StCDPK1* (PGSC0003DMG400027877) is strongly expressed in callus, stolons, petioles and roots, to a lesser extent in shoots and leaves and at very low levels in sepals and stamens suggesting that this kinase is quite ubiquitous. On the other hand, Northern blot and semi-quantitative RT-PCR assays indicated that it was strongly expressed in swollen stolons (Gargantini et al. 2009, Raices et al. 2001, Raices et al. 2003c) and Western blot data with anti-CDPK1 antibody confirmed the presence of the protein in swollen stolons (Gargantini et al. 2009). In order to

This article is protected by copyright. All rights reserved.

Accepted Article

perform a spatial analysis of *StCDPK1* expression, CDPK1pro::GUS plants were developed. Fourteen independent lines were obtained and those with highest GUS activity (lines J, K and N) were selected for histochemical analysis (Appendix S3C). With different intensity, all lines presented a similar expression pattern, GUS activity being stronger in roots and in the upper portion of the stem (Appendix S3E).

As observed in Fig. 1A, GUS activity was evident in stems and petioles of CDPK1pro::GUS plants. Stem cross sections revealed that GUS activity was restricted to the epidermis and to the vascular bundles (Fig. 1B), while no staining was observed in control plants (Fig. 1C). GUS activity was also observed in the midrib and leaf veins but not in the leaf blade (Fig. 1D and E). In accordance with the regulatory elements related to expression in roots, GUS activity was very strong in root vascular tissues of primary and secondary roots from soil and in vitro grown plants (Fig. 1F and G), in root hairs (Fig. 1I), and in aerial roots developing from in vitro plants (Fig. 1J). However, no staining was observed in the root cap (Fig. 1H). GUS activity was evident in axillary buds (Fig. 1K) but not in the shoot apex (Fig. 1L).

CDPK1pro::GUS plants were cultured in vitro under tuber inducing conditions in order to obtain the different tuberization stages (Fig. 2A). The first modification related to tuber formation was the bending of the subapical portion of the stolon (stage 1, S1). GUS activity was localized in the subapical portion of thin and cylindrical early stolons (ES) and in S1, (Fig. 2B and C). Longitudinal sections of S1 confirmed that GUS activity was strong in the vascular tissue dividing the external cortical parenchyma from the internal medullar parenchyma (Fig. 2D). S1 stolons from soil grown CDPK1pro::GUS plants presented a similar expression pattern (data not shown). As shown in Fig. 2E, GUS activity was low in stage 2 stolons (S2), while it was induced again in swollen stolons (stage 3, S3). In S3, both the vascular ring (Fig. 2F) and the mono-stratified epidermis of isodiametric cells (Fig. 2G and H) displayed intense GUS staining. However, in in vitro grown mature mini-tubers with a pluristratified peridermis, GUS activity was restricted to tuber eyes (Fig. 2I, J and K) and to the vascular system (Fig. 2L). Strong GUS staining was also observed in the stem-end of the tuber (Fig. 2M and N) while no activity was observed in the parenchymatic cells that accumulate starch.

In dormant tubers obtained from soil-grown plants (in a more advanced stage of development) GUS activity was evident only in the vascular ring as observed in the longitudinal and transverse tuber cuts (Fig. 2O and P), no GUS activity was observed in the peridermis or in dormant tuber eyes (Fig 2Q). After the end of the dormancy period, GUS activity was again intense in sprouting tuber eyes and in the developing sprouts (Fig. 2R, S and T). Overall, StCDPK1 promoter displays a dynamic pattern in a tissue specific manner throughout the potato vegetative life cycle.

miR390 in potato

In order to analyze if potato miRNAs could target StCDPK1, a detailed in silico search was conducted

This article is protected by copyright. All rights reserved.

Accepted Article

using the transcript sequence of StCDPK1 as target. The online tool psRNATarget predicted that *miR390* (21 bp) could target StCDPK1 mRNA in the Kinase Domain (KD) arresting its translation (expectation values and sequence alignments are shown in Fig. 3A). The same search was validated with TargetAlign software as well (data not shown). *miR390* is the only member of this conserved family in potato (Lakhotia et al. 2014). The secondary structure of *miR390* precursor (GenBank Accession CK247568.1) was predicted by MFold (Zuker 2003). It showed a typical hairpin loop secondary structure with mature *miR390* sequence in its stem region, a characteristic of miRNA precursors (Fig. 3B). The presence of the precursor (835 bp) was detected by RT-PCR in leaves, whereas the mature *miR390* (21 bp) was confirmed by stem-loop RT-PCR in whole plants and stolons of *S. tuberosum* ssp. *andigena* and *S. tuberosum* ssp. *tuberosum* (Fig. 3C and D).

The precursor sequence was then blasted (blastn) against the PGSC *S. tuberosum* group Phureja DM1-3 scaffold (v3), superscaffold (v3) and Pseudomolecules (v4.03; v2.1.11; v2.1.10) databases and against ITAG *Solanum lycopersicum* pseudomolecules (v2.3) database. According to Pseudomolecule Tilling Path (v4.03) database the best hit was chr10 position 49608938 to 49609772 (100% identical, E value 0.0), which corresponds to PGSC0003DMS000001874 in scaffold (v3) or to PGSC0003DMS000000664 in superscaffold (v3) databases. The other hits only cover a small portion of the amplicon (Appendix S6A). In tomato, the best hit was SL2.40ch10 (top query coverage: 27.19; Identity 92.21), interestingly the region that contains the mature microRNA sequence was 100% identical (Appendix S6B).

The 100 kb genomic region surrounding *miR390* precursor contains ten genes (Appendix S6C); the nearest upstream gene, a gene of unknown function, is 2.6 kb apart and the nearest downstream gene encoding a Brassinazole-resistant 2 protein, is 19.3 kb apart. The orientation of transcription of both neighboring genes is opposite to *miR390* precursor transcription. The 2 kb region upstream of *miR390* precursor was analyzed searching for *cis*-elements that could modulate its expression and that were also present in *StCDPK1* promoter. *miR390* precursor upstream region contains even more elements that drive expression of storage proteins than StCDPK1 promoter, and also presents root specific and cytokinins-responsive elements, although less than StCDPK1 promoter (Table 1, Appendix S5B); however, it does not contain AC elements. While *miR390* precursor promoter shares with *StCDPK1* promoter most of the elements responsive to osmotic, drought, and salinity stress, it presents few light-responsive elements (Appendix S5B). In addition, the *miR390* precursor promoter contains elements responsive to auxin (1 AUXRETGA1GMGH3, P =1.79E-05 and 1 AuxRR-core, P =5.35E-05), ethylene (1 ERE, P =2.65. E-05) and ABA (1 ABREMOTIFAOSOSEM, P =1.47. E-05).

This article is protected by copyright. All rights reserved.

Accepted Article

Posttranscriptional regulation of StCDPK1 by *miR390*

In order to analyze StCDPK1 and *miR390* expression at the transcript level, qRT-PCR of different tissues was carried out. As can be observed (Fig. 4), *miR390* and *StCDPK1* are expressed in the same tissues but their relative transcription pattern is quite different. Compared to other tissues, *miR390* and StCDPK1 displayed an inverse expression in leaves and in tuber eyes (Fig. 4, *P*-values are shown in Appendix S7). *StCDPK1* transcripts were ubiquitously expressed in all tissues (Fig. 4A) following a spatio-temporal profile as observed in CDPK1pro::GUS plants (Fig. 1 and 2). Western blot analysis confirmed this result in most tissues; however StCDPK1 protein was not detected in leaves (Fig.4B). A possible explanation to this discrepancy is that, according to GUS plants, *StCDPK1* expression was restricted to leaf veins. However, the high expression of miR390 in leaves could suggest that *miR390* affects the kinase expression posttranscriptionally in these organs. On the other hand, StCDPK1 protein was detected in tuber eyes where a high expression of miR390 was also observed. Since qRT-PCR and Western blot analysis were performed with different samples of tuber eyes, it is possible that the dormancy status of both samples was different.

In order to validate the posttranscriptional regulation of *StCDPK1* by *miR390*, generation of 35S::StCDPK1 and 35S::miR390 precursor constructs was performed and transient co-expression experiments in *N. benthamiana* were carried out. qRT-PCR assays confirmed the expression of *StCDPK1* and of the mature *miR390* in the agroinfiltrated leaves (Fig. 5). As observed, *StCDPK1* and *miR390* transcript levels were significantly enhanced relative to controls or EV treatments (Fig. 5A and B). When co-agroinfiltrations were performed with both CDPK1 and the precursor constructs, transcript levels of *StCDPK1* sharply declined (Fig 5A), while *miR390* levels were not affected (Fig. 5B). StCDPK7 is a CDPK isoform that belongs to group 1 and that was not predicted as target of *miR390*. In order to determine if the StCDPK1-*miR390* interaction was specific, co-agroinfiltration of the *miR390* precursor together with *StCDPK7* was also performed (Fig. 5C). In this case, no significant reduction in *StCDPK7* transcript levels was observed. In addition, Western blot analysis of agroinfiltrated leaves was performed using anti-His antibody to detect StCDPK1-6xHis or StCDPK7-6xHis. A specific band was detected in leaves expressing the CDPK1-6xHis protein indicating that the mRNA was translated (Fig. 5D). However, correlating with the qRT-PCR results, this band was not observed in the control of un-infiltrated leaves, in leaves agroinfiltrated with the precursor or with EV, or in leaves co-agroinfiltrated with both the precursor and *StCDPK1*. On the other hand, StCDPK7 protein levels were not affected by the microRNA (Fig. 5D). Altogether, these results strongly suggest that *miR390* specifically targets *StCDPK1* transcripts at the posttranscriptional level.

This article is protected by copyright. All rights reserved.

Accepted Article

In vitro phosphorylation of StPIN4 by StCDPK1

In stolons and tubers, GUS activity driven by *StCDPK1* promoter overlaps with the high auxin concentration visualized in the auxin responsive promoter DR5::GUS plants (Roumeliotis et al. 2012a). In addition, *StCDPK1* displays a similar expression pattern in the vascular tissue of stolons and tubers as the long looped PINs, *StPIN4* and *StPIN2* (Roumeliotis et al. 2013). *StCDPK1* shares with *StPIN4*, the expression in the subapical region where the swelling of the stolon takes place and in the basal part of the pith close to the heel of the tuber, where it attaches the stolon. It was reported that the polar localization of PIN proteins is controlled by reversible phosphorylation of the PIN hydrophilic loop (Armengot et al. 2016, Huang et al. 2010, Sasayama et al. 2013). StPIN4 conserves the M3 motif and two TPRXS(N/S) motifs (Appendix S4C) reported to be phosphorylated in AtPINs (Huang et al. 2010, Sasayama et al. 2013). An in silico search performed with NetPhos.2 (Blom et al. 1999) predicted other phosphorylation sites in StPIN4 hydrophilic loop, among which are nine serines and three threonine with scores higher than 0.95 (Appendix S4D). These phosphorylation sites could be targeted by different kinases; a possible candidate is StCDPK1, an active plasma membrane-associated kinase (Gargantini et al. 2009, Raices et al. 2003c).

In order to analyze if StCDPK1 could phosphorylate the hydrophilic loop of StPIN4, the recombinant protein StPIN4HL tagged with 6xHis was produced (Appendix S4B). A phosphorylation assay using a constant amount of StCDPK1-6xHis as enzyme source and increasing amounts of StPIN4HL-6xHis (0.25–2 µg) as substrate, showed that StPIN4 was phosphorylated in a calcium dependent manner by StCDPK1 (Fig. 6A). Noticeably, StCDPK1 autophosphorylation increased concomitantly with the amount and phosphorylation of StPIN4HL-6xHis, being highest at 2 µg (Fig. 6a). Additionally, StCDPK1 autophosphorylation was assayed in the absence of substrates or in the presence of the tobacco NtPAL3-6xHis recombinant protein (0.5 µg) (Fig. 6B). It was reported that AtCPK1 phosphorylates a poplar PAL (Allwood et al. 1999, Cheng et al. 2001), however StCDPK1 was unable to phosphorylate the tobacco NtPAL3-6xHis. The phosphorylated band observed in Fig. 6B corresponds to StCDPK1 calcium dependent autophosphorylation. Based on our data, we can conclude that, in vitro StPIN4HL is a specific substrate for StCDPK1, and that the kinase undergoes calcium dependent autophosphorylation either in the presence of a phosphate acceptor such as PIN, in the presence of a protein that it cannot phosphorylate or in the absence of any substrate. In order to further study the autophosphorylation of the kinase, StCDPK1 recombinant protein was incubated with cold ATP and calcium and was analyzed by 2D Western blot developed with anti-polyhistidine antibody. As can be observed in Fig. 6C, the signal detected at the estimated molecular weight of the kinase (60 kDa) spanned different isoelectric points correlating with a protein phosphorylated in multiple sites. According to NetPhos.2 analysis, there are eight serines (scores>0.95) in StCDPK1 protein sequence that could be potential autophosphorylation sites

This article is protected by copyright. All rights reserved.

Accepted Article

(Appendix S4D).

Discussion

StCDPK1 promoter and transcription profile

Extensive research conducted in different plant species has provided conclusive evidence that CDPKs are central regulators of Ca^{2+}-mediated processes in response to environmental challenges. Some CDPKs are found to have ubiquitous expression pattern, whereas others are tissue-specific (Boudsocq and Sheen 2013). Both in Arabidopsis and rice, distinct CDPK isoforms represent crucial signaling nodes that mediate plant responses to both biotic and abiotic signals (Boudsocq and Sheen 2013). More recent reports indicate the role of specific CDPKs in developmental processes like pollen tube growth (Gutermuth et al. 2013, Myers et al. 2009, Zhou et al. 2014), stem elongation (Matschi et al. 2013), cotton fiber elongation (Huang et al. 2008) and in rice grain filling (Manimaran et al. 2015). In Arabidopsis CDPK isoforms were shown to act on root hydraulic conductivity (Li et al. 2015), root growth (Luo et al. 2014) and root gravitropism (Huang et al. 2013).

Previous results from our group showed that StCDPK1 was involved in tuber development (Gargantini et al. 2009, Raices et al. 2001, Raices et al. 2003c). In the current study, we thoroughly analyzed the transcription profile of *StCDPK1* in different plant tissues and throughout the potato vegetative life cycle. Though not directly comparable (sampling was done on different genotypes, time courses and tissue types), the qRT-PCRs results from our investigation and the RNA-seq data available at the potato genome database indicated that *StCDPK1* is ubiquitously expressed in all plant tissues (Fig.5). CDPK1pro::GUS plants confirmed that *StCDPK1* exhibited a dynamic spatio-temporal expression pattern throughout tuber development, dormancy and sprouting, and strongly indicate that it is mainly associated with the vascular tissues in leaves, stems and roots (Figs 1 and 2). When comparing GUS activity in CDPK1pro::GUS plants with that of CDPK3pro::GUS plants (Grandellis et al. 2012), the expression profile was found to be clearly different and StCDPK3 does not appear to be associated with the vascular tissue. Both promoters are active during the different stages of tuber development but display a different spatio-temporal expression profile, which is possibly related to their distinct roles during tuberization.

Stronger GUS activity was observed in the upper part of the stem, where elongation takes place, and in the sub-apical portion of elongating early stolons and sprouts (Appendix S3, Fig. 2). Strikingly, CDPK1prom::GUS lines share a very similar profile with the CPK28 isoform reported to be a regulatory component that controls stem elongation and vascular development in *Arabidopsis thaliana*. In cross-sections of the inflorescence stem, CPK28 promoter activity was localized exclusively to the xylem (Matschi et al. 2013). Our GUS activity results (Figs 1 and 2), together with the presence of an AC element in StCDPK1 promoter (Table 1) support the expression of StCDPK1 in xylem. AC elements are

This article is protected by copyright. All rights reserved.

Accepted Article

associated with genes related to G lignin biosynthesis (Raes et al. 2003), a polymer present in xylem vessels (Donaldson 2001). Apart from StCDPK1 only four isoforms of the *S. phureja* CDPK family (PGSC0003DMG400025808, DMG400013183, DMG400009451, DMG400005829) contain the AC element in their promoters. GA is involved in shoot and stolon elongation by promoting fiber elongation and general xylogenesis (Eriksson et al. 2000, Israelsson et al. 2003, Mauriat and Moritz 2009). According to our results, we could suggest that StCDPK1 may be involved in stem elongation. This hypothesis is supported by our previous findings with transgenic plants with reduced *StCDPK1* expression in tuberization stages; upon treatment with GA, transgenic stolons were significantly shorter than those of control plants (Gargantini et al. 2009).

The presence of stress-responsive elements associated with ABA, drought and salinity in *StCDPK1* promoter (Table 1, Appendix S5B) correlates with the role of CDPKs as sensor/transducers of abiotic stimuli (Boudsocq et al. 2010, Campo et al. 2014, Franz et al. 2011, Romeis 2001, Xu et al. 2010, Zhu et al. 2007). In the future, it would be interesting to analyze if StCDPK1 is involved in the plant´s response to abiotic stresses.

Posttranscriptional regulation of StCDPK1 by *miR390*

Several molecules co-exist in the vascular system of plants; among them are miRNAs that represent an additional layer in the regulation of gene expression affecting various developmental processes. For example, ATHB15 seems to negatively affect xylem development, while *miR166*-mediated cleavage of ATHB15 transcript promotes xylem differentiation (Kim et al. 2005). Whether miRNAs could play a role regulating a CDPK at a posttranscriptional level was not known. In this report, we show for the first time that StCDPK1 is regulated by *miR390*.

Through in silico analysis and deep sequencing approaches of small RNA libraries prepared from tissues of leaf, root, stem and four developmental stages of potato tuber, conserved miRNA families and potato specific miRNAs were identified (Lakhotia et al. 2014, Zhang et al. 2013). While most of the potato miRNA targets were found to be transcription factors, it was predicted that *miR390* could target both a protein phosphatase and a kinase (Lakhotia et al. 2014). Our in silico search using StCDPK1 transcript sequence in two different on-line tools, predicted that StCDPK1 was targeted by *miR390*, and due to the extent of complementarity between them it was predicted that the regulation was at translational level (Fig. 4A). Interestingly, the sequence targeted by *miR390* corresponds to the KD (Kinase Domain) in a region that is quite conserved among CDPKs suggesting that it could be a general mode of regulation. However, when the transcript sequences of other CDPKs identified in our laboratory, StCDPK2 (AF418563.3), StCDPK3 (AF518003) and StCDPK7 (KJ830932), were used as targets, the on-line tool retrieved no positive results suggesting that StCDPK1 is a specific target of *miR39* among CDPKs. We

This article is protected by copyright. All rights reserved.

Accepted Article

cannot exclude that miR390 may have other targets whose expression pattern may match with miR390 expression.

Analysis of *miR390* precursor promoter sequence revealed the presence of numerous *cis*-elements related to expression in roots and storage proteins, as well as cytokinin and stress responsive elements, all of which are also present in *StCDPK1* promoter (Table 1, Appendix S5B). The similarities between both promoters could imply that, under certain conditions, *StCDPK1* and the *miR390* precursor are simultaneously transcribed. Although Lakhotia et al (2014) analyzed the expression of 15 conserved and 6 specific potato miRNAs in different potato tissues and in early tuberization stages, *miR390* was not among them. The presence of both the mature form and the *miR390* precursor was confirmed in whole plant tissues and stolons (Fig. 4C and D). In addition, qRT-PCR analysis (Fig. 5) revealed that *miR390* was expressed in all the examined potato plant tissues but its expression was significantly higher in leaves and in tuber eyes from dormant tubers. It is noteworthy that StCDPK1 and *miR390* transcript levels exhibit opposite expression profiles in these two organs, indicating a possible miR390-mediated regulation of StCDPK1. Moreover, StCDPK1 protein levels in leaves did not correlate with transcript levels.

In tubers of a secondary developmental state, the epidermis is replaced by a suberized periderm (Reeve et al. 1969). The periderm is initiated by divisions of both the epidermal and subepidermal cells, first at the stem end and later in the bud-end region of the tuber (Artschwager 1924, Reeve et al. 1969). During the early stage of periderm development in swollen stolons, when the phellogen is actively dividing, StCDPK1 promoter activity was evident; however, it sharply declined in the pluristratified peridermis of in vitro mini-tubers remaining only in tuber eyes. However, in dormant tubers from soil-grown plants GUS activity was not detected in tuber eyes; it was observed only after dormancy break when sprouting initiated (Fig. 2). It is tempting to suggest that *miR390* could be involved in controlling StCDPK1 expression in dormant tubers; *miR390* could reduce its presence in tuber eyes but not in the vascular ring.

The drastic decrease of StCDPK1 transcripts and protein levels observed upon co-agroinfiltration with *mi390* (Fig. 5A and D), demonstrated that *miR390* regulates the kinase expression posttranscriptionally. Although in silico analysis predicted translational inhibition as the mode of action of *miR390*, we show that *miR390* targets StCDPK1 transcripts as well. This finding is in accordance with the recent understanding of miRNA target gene regulation that it can function at both, transcriptional cleavage and translational arrest (Brodersen et al. 2008, Liu et al. 2014). The fact that CDPKs could be controlled posttranscriptionally adds a new layer of control to these versatile kinases. Future work will help to elucidate the role of *miR390* in potato tuberization, dormancy and sprouting.

This article is protected by copyright. All rights reserved.

Accepted Article

StPIN4 could be a downstream target of StCDPK1

Auxin´s effect on growth strongly correlates with cortical microtubules arrangements (Nick et al. 1992). The changes in the orientation of cell division that result in swelling of the stolon tip could be compatible with a role for auxin in tuber development. At the onset of tuberization, auxin content increases locally in the stolon tip just prior to stolon swelling correlating with a peak in the expression of a *StYUC* gene and the main direction of IAA movement is from the stolon tip to the basal part of the stolon (Roumeliotis et al. 2012a). PIN transporters are responsible for the generation of auxin gradients and the establishment of auxin maxima and minima that are critical for organ patterning (Finet and Jaillais 2012).

Reversible phosphorylation of the PIN hydrophilic loop controls the polar localization of these auxin transporters (Armengot et al. 2016, Huang et al. 2010, Sasayama et al. 2013). CRK5, a member of the Ca^{2+}/calmodulin-dependent kinase-related protein family is required for proper polar localization of AtPIN2 in the transition zones of roots (Ganguly et al. 2014, Rigo et al. 2013). StPIN4-HL presents several phosphorylation sites (Fig. S2) that could be targeted by different kinases to confer different localization cues in a cell type-specific manner. In vitro, StCDPK1 was able to phosphorylate the hydrophilic loop of StPIN4 in a calcium dependent manner (Fig. 6). While further in vivo studies are required to confirm that StPIN4 is a target of StCDPK1, StCDPK1 association with the plasma membrane (Raíces et al. 2003, Gargantini et al. 2009) and its similar expression pattern in the vascular tissue of stolons and tubers as StPIN4 and StPIN2 (Roumeliotis et al. 2013) allows us to consider this hypothesis. It would be interesting to know if this kinase plays a role in controlling auxin flux during stolon to tuber transition. In summary, our experiments and results indicate that *StCDPK1* expression is varied in tissue specific manner throughout the potato life cycle having a significant expression in the vasculature, it is targeted by miR390 at posttranscriptional level and suggest that StPIN4 is one of its downstream targets revealing the overall role of this kinase in potato development.

Author contributions

FS produced and characterized the CDPK1pro::GUS plants, produced StCDPK1 and StPIN4 recombinant proteins and conducted phosphorylation assays; cloned miR390 precursor; produced the S35pro::StCDPK1-6xHis and the S35pro::miR390pre constructs and performed co-agroinfiltration assays and the corresponding Western blot analysis. SB performed the in silico analysis of miR390 targets, identified the miR390 precursor, its secondary structure and the qRT-PCR from the different tissues for miR390 and stCDPK1.EF produced the S35pro::StCDPK7-6xHis construct, performed the qRT-PCRs of the co-agroinfitration assays and the 2D gel electrophoresis assay. CG cloned the StCDPK1 promoter using the Genome Walker kit. RU cloned the mature form of miR390. Bioinformatic analysis was conducted by FS, CG, SB and RU. RU and AKB conceived, designed and discussed the experiments and

This article is protected by copyright. All rights reserved.

Accepted Article

wrote the manuscript. All authors read and approved the manuscript.

Acknowledgements – This work was supported by grants from the Consejo Nacional de Investigaciones Científicas y Técnicas (CONICET), the University of Buenos Aires (UBA), Argentina, and the bilateral INDO-ARGENTINE S & T COOPERATION PROGRAMME, Ministerio de Ciencia y Tecnología MINCYT, Argentina; Department of Science and Technology (DST), Government of India, New Delhi. RMU is member of the National Research Council, CONICET and Associate Professor at UBA. FS, EF, and CG are fellows from CONICET. AKB is an Associate Professor at the Indian Institute of Science Education and Research (IISER) Pune; SB is a senior research fellow from IISER Pune, India.

References

Allwood EG, Davies DR, Gerrish C, Ellis BE, Bolwell GP (1999) Phosphorylation of phenylalanine ammonia-lyase: evidence for a novel protein kinase and identification of the phosphorylated residue. FEBS Lett 457: 47–52

Armengot L, Marques-Bueno MM, Jaillais Y (2016) Regulation of polar auxin transport by protein and lipid kinases. J Exp Bot 67: 4015–4037

Artschwager EF (1924) Studies on the potato tuber. J Agricult Res 27: 809–836

Balamani V, Veluthambi K, Poovaiah BW (1986) Effect of Calcium on Tuberization in Potato (*Solanum tuberosum* L.). Plant Physiol 80: 856–858

Baskin TI (2015) Auxin inhibits expansion rate independently of cortical microtubules. Trends Plant Sci 20: 471–472

Bhogale S, Mahajan AS, Natarajan B, Rajabhoj M, Thulasiram HV, Banerjee AK (2014) MicroRNA156: a potential graft-transmissible microRNA that modulates plant architecture and tuberization in *Solanum tuberosum* ssp. *andigena*. Plant Physiol 164: 1011–1027

Blom N, Gammeltoft S, Brunak S (1999) Sequence and structure-based prediction of eukaryotic protein phosphorylation sites. J Mol Biol 294: 1351–1362

Boudsocq M, Sheen J (2013) CDPKs in immune and stress signaling. Trends Plant Sci 18: 30–40

Boudsocq M, Willmann MR, McCormack M, Lee H, Shan L, He P, Bush J, Cheng SH, Sheen J (2010) Differential innate immune signalling via Ca(2+) sensor protein kinases. Nature 464: 418–422

Brodersen P, Sakvarelidze-Achard L, Bruun-Rasmussen M, Dunoyer P, Yamamoto YY, Sieburth L, Voinnet O (2008) Widespread translational inhibition by plant miRNAs and siRNAs. Science 320: 1185–1190

Campo S, Baldrich P, Messeguer J, Lalanne E, Coca M, San Segundo B (2014) Overexpression of a Calcium-Dependent Protein Kinase Confers Salt and Drought Tolerance in Rice by Preventing Membrane Lipid Peroxidation. Plant Physiol 165: 688–704

This article is protected by copyright. All rights reserved.

Accepted Article

Chen C, Ridzon DA, Broomer AJ, Zhou Z, Lee DH, Nguyen JT, Barbisin M, Xu NL, Mahuvakar VR, Andersen MR, Lao KQ, Livak KJ, Guegler KJ (2005) Real-time quantification of microRNAs by stem-loop RT-PCR. Nucleic Acids Res 33: e179

Chen X, Grandont L, Li H, Hauschild R, Paque S, Abuzeineh A, Rakusova H, Benkova E, Perrot-Rechenmann C, Friml J (2014) Inhibition of cell expansion by rapid ABP1-mediated auxin effect on microtubules. Nature 516: 90–93

Chen X, Wu S, Liu Z, Friml J (2016) Environmental and Endogenous Control of Cortical Microtubule Orientation. Trends Cell Biol 26: 409–419

Cheng SH, Sheen J, Gerrish C, Bolwell GP (2001) Molecular identification of phenylalanine ammonia-lyase as a substrate of a specific constitutively active Arabidopsis CDPK expressed in maize protoplasts. FEBS Lett 503: 185–188

Cutter EG (1978) Structure and development of the potato plant. In: Harris PM (ed), The Potato Crop: The Scientific Basis For Improvement. Chapman & Hall, London. pp 70–152

Dai X, Zhao PX (2011) psRNATarget: a plant small RNA target analysis server. Nucleic Acids Res 39: 155–159

Donaldson LA (2001) Lignification and lignin topochemistry – an ultrastructural view. Phytochemistry 57: 859–873

Dutt M, Dhekney SA, Soriano L, Kandel R, Grosser JW (2014) Temporal and spatial control of gene expression in horticultural crops. Hortic Res 1: 14047

Eriksson ME, Israelsson M, Olsson O, Moritz T (2000) Increased gibberellin biosynthesis in transgenic trees promotes growth, biomass production and xylem fiber length. Nat Biotechnol 18: 784–788

Finet C, Jaillais Y (2012) Auxology: when auxin meets plant evo-devo. Dev Biol 369: 19–31

Franz S, Ehlert B, Liese A, Kurth J, Cazale AC, Romeis T (2011) Calcium-dependent protein kinase CPK21 functions in abiotic stress response in *Arabidopsis thaliana*. Mol Plant 4: 83–96

Ganguly A, Park M, Kesawat MS, Cho HT (2014) Functional Analysis of the Hydrophilic Loop in Intracellular Trafficking of Arabidopsis PIN-FORMED Proteins. Plant Cell 26: 1570–1585

Gargantini PR, Giammaria V, Grandellis C, Feingold SE, Maldonado S, Ulloa RM (2009) Genomic and functional characterization of StCDPK1. Plant Mol Biol 70: 153–172

Giammaria V, Grandellis C, Bachmann S, Gargantini PR, Feingold SE, Bryan G, Ulloa RM (2011) StCDPK2 expression and activity reveal a highly responsive potato calcium-dependent protein kinase involved in light signalling. Planta 233: 593–609

Grandellis C, Giammaria V, Bialer M, Santin F, Lin T, Hannapel DJ, Ulloa RM (2012) The novel *Solanum tuberosum* calcium dependent protein kinase, StCDPK3, is expressed in actively growing organs. Planta 236: 1831–1848

This article is protected by copyright. All rights reserved.

Accepted Article

Grant CE, Bailey TL, Noble WS (2011) FIMO: scanning for occurrences of a given motif. Bioinformatics 27: 1017–1018

Gutermuth T, Lassig R, Portes MT, Maierhofer T, Romeis T, Borst JW, Hedrich R, Feijo JA, Konrad KR (2013) Pollen tube growth regulation by free anions depends on the interaction between the anion channel SLAH3 and calcium-dependent protein kinases CPK2 and CPK20. Plant Cell 25: 4525–4543

Harper JF, Sussman MR, Schaller GE, Putnam-Evans C, Charbonneau H, Harmon AC (1991) A calcium-dependent protein kinase with a regulatory domain similar to calmodulin. Science 252: 951–954

Hatton D, Sablowski R, Yung MH, Smith C, Schuch W, Bevan M (1995) Two classes of cis sequences contribute to tissue-specific expression of a PAL2 promoter in transgenic tobacco. Plant J 7: 859–876

Hauffe KD, Lee SP, Subramaniam R, Douglas CJ (1993) Combinatorial interactions between positive and negative cis-acting elements control spatial patterns of 4CL-1 expression in transgenic tobacco. Plant J 4: 235–253

Higo K, Ugawa Y, Iwamoto M, Korenaga T (1999) Plant cis-acting regulatory DNA elements (PLACE) database: 1999. Nucleic Acids Res 27: 297–300

Huang F, Zago MK, Abas L, van Marion A, Galvan-Ampudia CS, Offringa R (2010) Phosphorylation of conserved PIN motifs directs Arabidopsis PIN1 polarity and auxin transport. Plant Cell 22: 1129–1142

Huang QS, Wang HY, Gao P, Wang GY, Xia GX (2008) Cloning and characterization of a calcium dependent protein kinase gene associated with cotton fiber development. Plant Cell Rep 27: 1869–1875

Huang SJ, Chang CL, Wang PH, Tsai MC, Hsu PH, Chang IF (2013) A type III ACC synthase, ACS7, is involved in root gravitropism in *Arabidopsis thaliana*. J Exp Bot 64: 4343–4360

Israelsson M, Eriksson ME, Hertzberg M, Aspeborg H, Nilsson P, Moritz T (2003) Changes in gene expression in the wood-forming tissue of transgenic hybrid aspen with increased secondary growth. Plant Mol Biol 52: 893–903

Kim J, Jung JH, Reyes JL, Kim YS, Kim SY, Chung KS, Kim JA, Lee M, Lee Y, Narry Kim V, Chua NH, Park CM (2005) microRNA-directed cleavage of ATHB15 mRNA regulates vascular development in Arabidopsis inflorescence stems. Plant J 42: 84–94

Kloosterman B, Abelenda JA, Gomez Mdel M, Oortwijn M, de Boer JM, Kowitwanich K, Horvath BM, van Eck HJ, Smaczniak C, Prat S, Visser RG, Bachem CW (2013) Naturally occurring allele diversity allows potato cultivation in northern latitudes. Nature 495: 246–250

Kloosterman B, De Koeyer D, Griffiths R, Flinn B, Steuernagel B, Scholz U, Sonnewald S, Sonnewald U, Bryan GJ, Prat S, Banfalvi Z, Hammond JP, Geigenberger P, Nielsen KL, Visser RG, Bachem CW (2008) Genes driving potato tuber initiation and growth: identification based on transcriptional

This article is protected by copyright. All rights reserved.

Accepted Article

changes using the POCI array. Funct Integr Genomics 8: 329–340

Lakhotia N, Joshi G, Bhardwaj AR, Katiyar-Agarwal S, Agarwal M, Jagannath A, Goel S, Kumar A (2014) Identification and characterization of miRNAome in root, stem, leaf and tuber developmental stages of potato (*Solanum tuberosum* L.) by high-throughput sequencing. BMC Plant Biol 14: 6

Lescot M, Dehais P, Thijs G, Marchal K, Moreau Y, Van de Peer Y, Rouze P, Rombauts S (2002) PlantCARE, a database of plant cis-acting regulatory elements and a portal to tools for in silico analysis of promoter sequences. Nucleic Acids Res 30: 325–327

Li G, Boudsocq M, Hem S, Vialaret J, Rossignol M, Maurel C, Santoni V (2015) The calcium-dependent protein kinase CPK7 acts on root hydraulic conductivity. Plant Cell Environ 38: 1312–1320

Liu Q, Wang F, Axtell MJ (2014) Analysis of complementarity requirements for plant microRNA targeting using a *Nicotiana benthamiana* quantitative transient assay. Plant Cell 26: 741–753

Liu W, Stewart CN, Jr. (2016) Plant synthetic promoters and transcription factors. Curr Opin Biotechnol 37: 36–44

Livak KJ, Schmittgen TD (2001) Analysis of relative gene expression data using real-time quantitative PCR and the 2(–Delta Delta C(T)) Method. Methods 25: 402–408

Luo X, Chen Z, Gao J, Gong Z (2014) Abscisic acid inhibits root growth in Arabidopsis through ethylene biosynthesis. Plant J 79: 44–55

MacIntosh GC, Ulloa RM, Raices M, Tellez-Inon MT (1996) Changes in Calcium-Dependent Protein Kinase Activity during in Vitro Tuberization in Potato. Plant Physiol 112: 1541–1550

Manimaran P, Mangrauthia SK, Sundaram RM, Balachandran SM (2015) Constitutive expression and silencing of a novel seed specific calcium dependent protein kinase gene in rice reveals its role in grain filling. J Plant Physiol 174: 41–48

Martin A, Adam H, Diaz-Mendoza M, Zurczak M, Gonzalez-Schain ND, Suarez-Lopez P (2009) Graft-transmissible induction of potato tuberization by the microRNA miR172. Development 136: 2873–2881

Matschi S, Werner S, Schulze WX, Legen J, Hilger HH, Romeis T (2013) Function of calcium-dependent protein kinase CPK28 of *Arabidopsis thaliana* in plant stem elongation and vascular development. Plant J 73: 883–896

Mauriat M, Moritz T (2009) Analyses of GA20ox- and GID1-over-expressing aspen suggest that gibberellins play two distinct roles in wood formation. Plant J 58: 989–1003

Murashige T, Skoog F (1962) A revised medium for rapid growth and bio assays with tobacco tissue cultures. Physiol Plant 15: 473–497

Myers C, Romanowsky SM, Barron YD, Garg S, Azuse CL, Curran A, Davis RM, Hatton J, Harmon AC, Harper JF (2009) Calcium-dependent protein kinases regulate polarized tip growth in pollen tubes.

This article is protected by copyright. All rights reserved.

Accepted Article

Plant J 59: 528–539

Nick P, Schafer E, Furuya M (1992) Auxin Redistribution during First Positive Phototropism in Corn Coleoptiles : Microtubule Reorientation and the Cholodny–Went Theory. Plant Physiol 99: 1302–1308

Potato Genome Sequencing C, Xu X, Pan S, Cheng S, Zhang B, Mu D, Ni P, Zhang G, Yang S, Li R, Wang J, Orjeda G, Guzman F, Torres M, Lozano R, Ponce O, Martinez D, De la Cruz G, Chakrabarti SK, Patil VU, Skryabin KG, Kuznetsov BB, Ravin NV, Kolganova TV, Beletsky AV, Mardanov AV, Di Genova A, Bolser DM, Martin DM, Li G, Yang Y, Kuang H, Hu Q, Xiong X, Bishop GJ, Sagredo B, Mejia N, Zagorski W, Gromadka R, Gawor J, Szczesny P, Huang S, Zhang Z, Liang C, He J, Li Y, He Y, Xu J, Zhang Y, Xie B, Du Y, Qu D, Bonierbale M, Ghislain M, Herrera Mdel R, Giuliano G, Pietrella M, Perrotta G, Facella P, O'Brien K, Feingold SE, Barreiro LE, Massa GA, Diambra L, Whitty BR, Vaillancourt B, Lin H, Massa AN, Geoffroy M, Lundback S, DellaPenna D, Buell CR, Sharma SK, Marshall DF, Waugh R, Bryan GJ, Destefanis M, Nagy I, Milbourne D, Thomson SJ, Fiers M, Jacobs JM, Nielsen KL, Sonderkaer M, Iovene M, Torres GA, Jiang J, Veilleux RE, Bachem CW, de Boer J, Borm T, Kloosterman B, van Eck H, Datema E, Hekkert B, Goverse A, van Ham RC, Visser RG (2011) Genome sequence and analysis of the tuber crop potato. Nature 475: 189–195

Raes J, Rohde A, Christensen JH, Van de Peer Y, Boerjan W (2003) Genome-wide characterization of the lignification toolbox in Arabidopsis. Plant Physiol 133: 1051–1071

Raices M, Chico JM, Tellez-Inon MT, Ulloa RM (2001) Molecular characterization of StCDPK1, a calcium-dependent protein kinase from *Solanum tuberosum* that is induced at the onset of tuber development. Plant Mol Biol 46: 591–601

Raices M, Gargantini PR, Chinchilla D, Crespi M, Tellez-Inon MT, Ulloa RM (2003a) Regulation of CDPK isoforms during tuber development. Plant Mol Biol 52: 1011–1024

Raices M, MacIntosh GC, Ulloa RM, Gargantini PR, Vozza NF, Tellez-Inon MT (2003b) Sucrose increases calcium-dependent protein kinase and phosphatase activities in potato plants. Cell Mol Biol 49: 959–964

Raices M, Ulloa RM, MacIntosh GC, Crespi M, Tellez-Inon MT (2003c) StCDPK1 is expressed in potato stolon tips and is induced by high sucrose concentration. J Exp Bot 54: 2589–2591

Reeve RM, Hautala E, Weaver ML (1969) Anatomy and compositional variation within potatoes. American Potato Journal 46: 361–373

Reichert AI, He XZ, Dixon RA (2009) Phenylalanine ammonia-lyase (PAL) from tobacco (*Nicotiana tabacum*): characterization of the four tobacco PAL genes and active heterotetrameric enzymes. Biochem J 424: 233–242

This article is protected by copyright. All rights reserved.

Accepted Article

Rigo G, Ayaydin F, Tietz O, Zsigmond L, Kovacs H, Pay A, Salchert K, Darula Z, Medzihradszky KF, Szabados L, Palme K, Koncz C, Cseplo A (2013) Inactivation of plasma membrane-localized CDPK-RELATED KINASE5 decelerates PIN2 exocytosis and root gravitropic response in Arabidopsis. Plant Cell 25: 1592–1608

Rodriguez-Falcon M, Bou J, Prat S (2006) Seasonal control of tuberization in potato: conserved elements with the flowering response. Annu Rev Plant Biol 57: 151–180

Romeis T (2001) Protein kinases in the plant defence response. Curr Opin Plant Biol 4: 407–414

Roumeliotis E, Kloosterman B, Oortwijn M, Kohlen W, Bouwmeester HJ, Visser RG, Bachem CW (2012a) The effects of auxin and strigolactones on tuber initiation and stolon architecture in potato. J Exp Bot 63: 4539–4547

Roumeliotis E, Kloosterman B, Oortwijn M, Visser RG, Bachem CW (2013) The PIN family of proteins in potato and their putative role in tuberization. Front Plant Sci 4: 524

Roumeliotis E, Visser RG, Bachem CW (2012b) A crosstalk of auxin and GA during tuber development. Plant Signal Behav 7: 1360–1363

Sasayama D, Ganguly A, Park M, Cho HT (2013) The M3 phosphorylation motif has been functionally conserved for intracellular trafficking of long-looped PIN-FORMEDs in the Arabidopsis root hair cell. BMC Plant Biol 13: 189

Ulloa RM, Capiati DA, Giammaria V (2012) Signal Transduction Mechanisms Involved in Potato Developmental Processes. In: Caprara C (ed) Potatoes: Production, Consumption and Health Benefits. Nova Science Publishers. pp 125–146

Valmonte GR, Arthur K, Higgins CM, MacDiarmid RM (2014) Calcium-dependent protein kinases in plants: evolution, expression and function. Plant Cell Physiol 55: 551–569

Varkonyi-Gasic E, Wu R, Wood M, Walton EF, Hellens RP (2007) Protocol: a highly sensitive RT-PCR method for detection and quantification of microRNAs. Plant Methods 3: 12

Viola R, Roberts AG, Haupt S, Gazzani S, Hancock RD, Marmiroli N, Machray GC, Oparka KJ (2001) Tuberization in potato involves a switch from apoplastic to symplastic phloem unloading. Plant Cell 13: 385–398

Xie F, Zhang B (2010) Target-align: a tool for plant microRNA target identification. Bioinformatics 26: 3002–3003

Xu J, Tian YS, Peng RH, Xiong AS, Zhu B, Jin XF, Gao F, Fu XY, Hou XL, Yao QH (2010) AtCPK6, a functionally redundant and positive regulator involved in salt/drought stress tolerance in Arabidopsis. Planta 231: 1251–1260

Xu X, van Lammeren AA, Vermeer E, Vreugdenhil D (1998) The role of gibberellin, abscisic acid, and sucrose in the regulation of potato tuber formation in vitro. Plant Physiol 117: 575–584

This article is protected by copyright. All rights reserved.

Accepted Article

Yang J, Zhang Y, Cui X, Yao W, Yu X, Cen P, Hodges SE, Fisher WE, Brunicardi FC, Chen C, Yao Q, Li M (2013) Gene profile identifies zinc transporters differentially expressed in normal human organs and human pancreatic cancer. Curr Mol Med 13: 401–409

Zhang R, Marshall D, Bryan GJ, Hornyik C (2013) Identification and characterization of miRNA transcriptome in potato by high-throughput sequencing. PLoS One 8: e57233

Zhou L, Lan W, Jiang Y, Fang W, Luan S (2014) A calcium-dependent protein kinase interacts with and activates a calcium channel to regulate pollen tube growth. Mol Plant 7: 369–376

Zhu SY, Yu XC, Wang XJ, Zhao R, Li Y, Fan RC, Shang Y, Du SY, Wang XF, Wu FQ, Xu YH, Zhang XY, Zhang DP (2007) Two calcium-dependent protein kinases, CPK4 and CPK11, regulate abscisic acid signal transduction in Arabidopsis. Plant Cell 19: 3019–3036

Zuker M (2003) Mfold web server for nucleic acid folding and hybridization prediction. Nucleic Acids Res 31: 3406–3415

Edited by E. Scarpella

This article is protected by copyright. All rights reserved.

Accepted Article

Figure legends

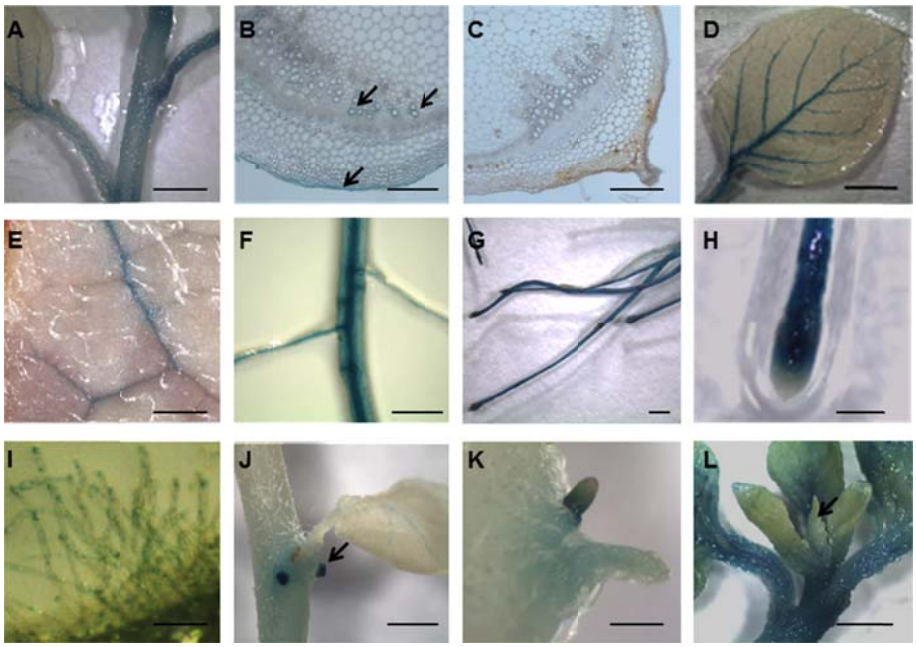

Fig. 1. GUS activity analysis in different tissues in CDPK1pro::GUS plants. (A) Stems and petioles. (B) Stem cross section of transgenic plant. Arrows indicate staining in epidermis and vascular tissue. (C) Stem cross section of control plant. (D) Leaf from in vitro grown plant. (E) Leaf from soil grown plant. (F) Root from soil grown plant. (G) Roots from in vitro grown plant. (H) Root cap. (I) Root hairs. (J) Adventitious roots (indicated by arrows). (K) Axillary buds. (L) Shoot apex (arrow indicates absence of GUS staining in this tissue). Bars = 2 mm in panels A, D, G, J, L; 1 mm in panels E, F; 500 µm in panels B, C, H; 100 µm panel I.

This article is protected by copyright. All rights reserved.

Accepted Article

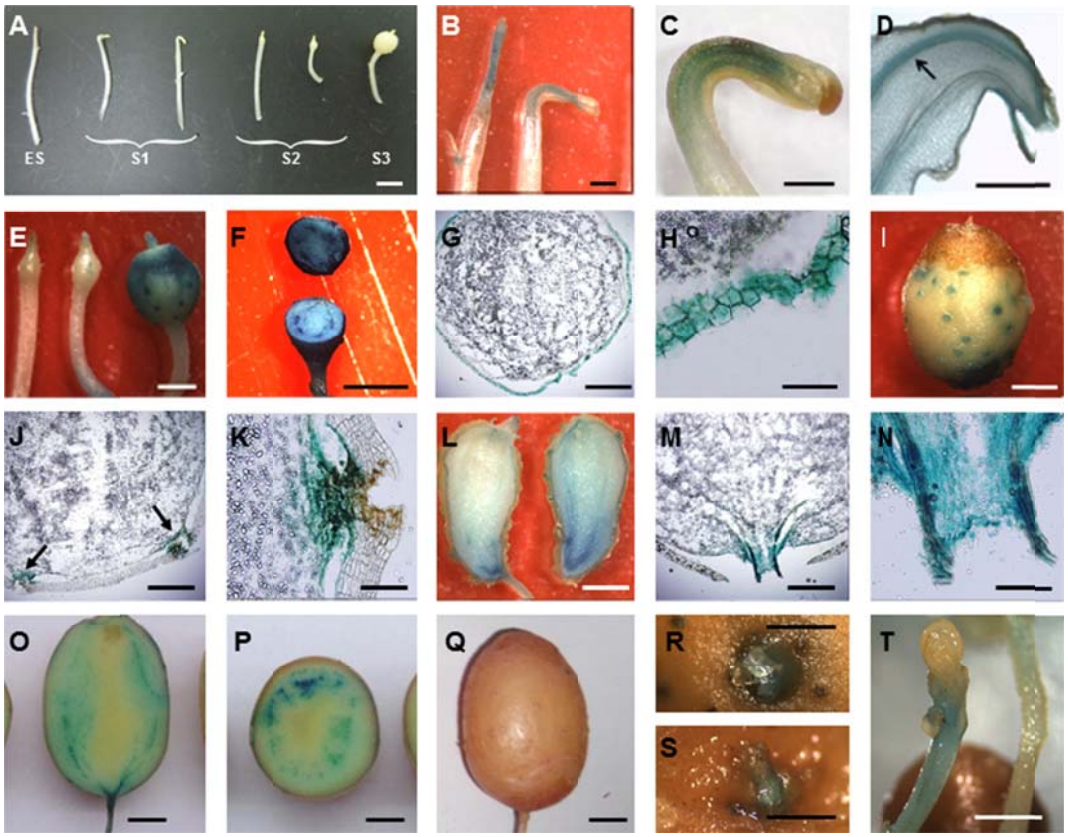

Fig. 2. GUS activity analysis of CDPK1pro::GUS plants during tuberization. (A) Tuberization stages. (B) Early stolon (ES) (left) and S1 stolon (right). (C) S1 stolon tip. (D) Longitudinal section of S1 stolon tip. (E) S2 stolons (left) and S3 stolon (right). (F) Transverse cut of S3 stolon. (G) Cross section of S3 stolon. (H) S3 stolon epidermal cells. (I) Mature tuber. (J) Cross section of mature tuber. (K) Tuber eye (L) Longitudinal cut of mature tuber. (M) Longitudinal section of mature tuber. (N) Vascular tissue in stem end of mature tuber. (O) Longitudinal cut of dormant tuber. (P) Transverse cut of dormant tuber. (Q) Dormant tuber. (R) Sprouting tuber eye at an early stage (S) Sprouting tuber eye at an advanced stage. (T) Tuber sprout. Bars = 1 cm in panels F, O, P, Q; 5 mm in panels A, F, I, L; 2.5 mm in panel E, T; 1 mm in panels B, C, G, J, M, R, S; 500 µm in panels D, K, N; 100 µm in panel H.

This article is protected by copyright. All rights reserved.

Accepted Article

A

psRNATarget prediction results	
miRNA Accession	Stu-*miR390*
Target Accession	gi|10568115|gb|AF115406.2
Expectation (E)	5.0
Target Accessibility (UPE)	15.05
Alignment	miRNA 21 CCACGAUAGGGAGGACUCGAA 1 :::::::: : :: ::: ::: Target 607 GGUGUUAUGCAUCGUGAUCUU 627
Target description	*Solanum tuberosum* calcium-dependent protein kinase mRNA cds
Inhibition	Translation
Multiplicity	1

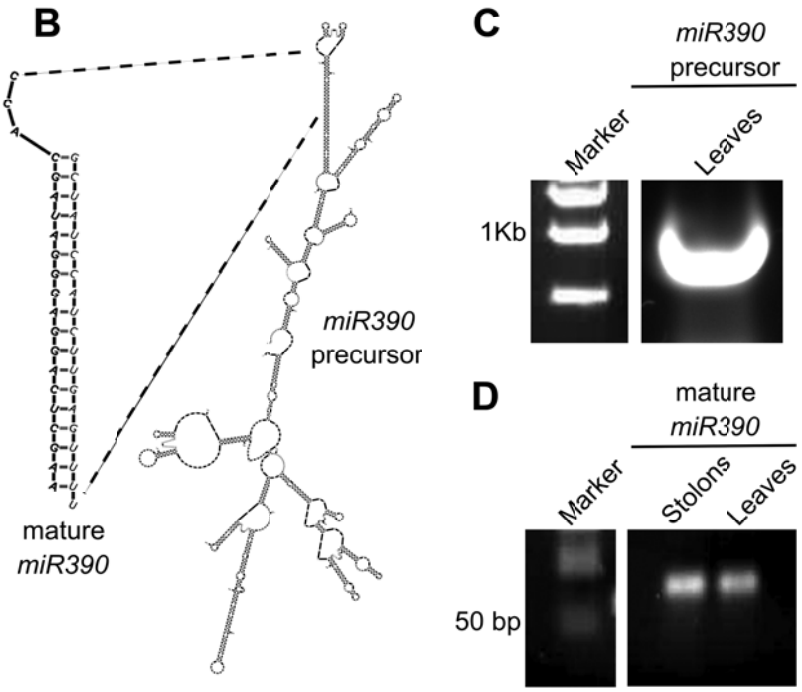

Fig. 3. Target prediction and validation of *miR390* in potato cultivar Desirée. (A) psRNATarget prediction results showing expectation values and sequence alignments (B) Secondary structure of *miR390* precursor as predicted by MFold (Zuker 2003). Mature *miR390* sequence is highlighted. (C) RT-PCR of *miR390* precursor in leaves. (d) Stem loop RT-PCR of mature *miR390* from stolons and leaves.

This article is protected by copyright. All rights reserved.

Accepted Article

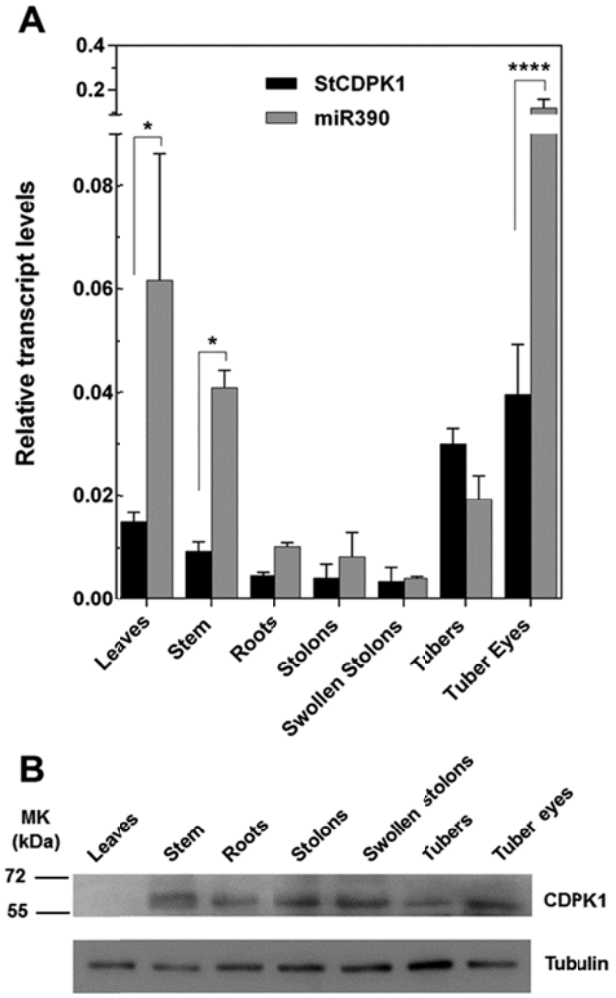

Fig. 4. Expression of *StCDPK1* and *miR390* in different tissues of potato plants. (A) qRT-PCRs performed in leaves, stem, roots, stolons, swollen stolons, dormant tubers and dormant tuber eyes from soil grown plants. GAPDH (Gylceraldehyde-3-phosphate dehydrogenase) was used for normalization. Error bars indicate (±) SD of three biological replicates each with three technical replicates. Data were analyzed with two-way ANOVA and Tukey's multiple comparison test ($P< 0.05$). Statistical significance between groups is indicated by * ($P<0.05$) and *** ($P<0.001$). The target exhibited significant inverse correlations with the miRNA in leaves and tuber eyes ($P=0.0079$ and $P<0.0001$ respectively). (B) Total protein extracts (50 µg) from the different tissues were subjected to Western blot analysis with anti-CDPK1 antibody (1:300). Tubulin was used as a loading control.

This article is protected by copyright. All rights reserved.

Accepted Article

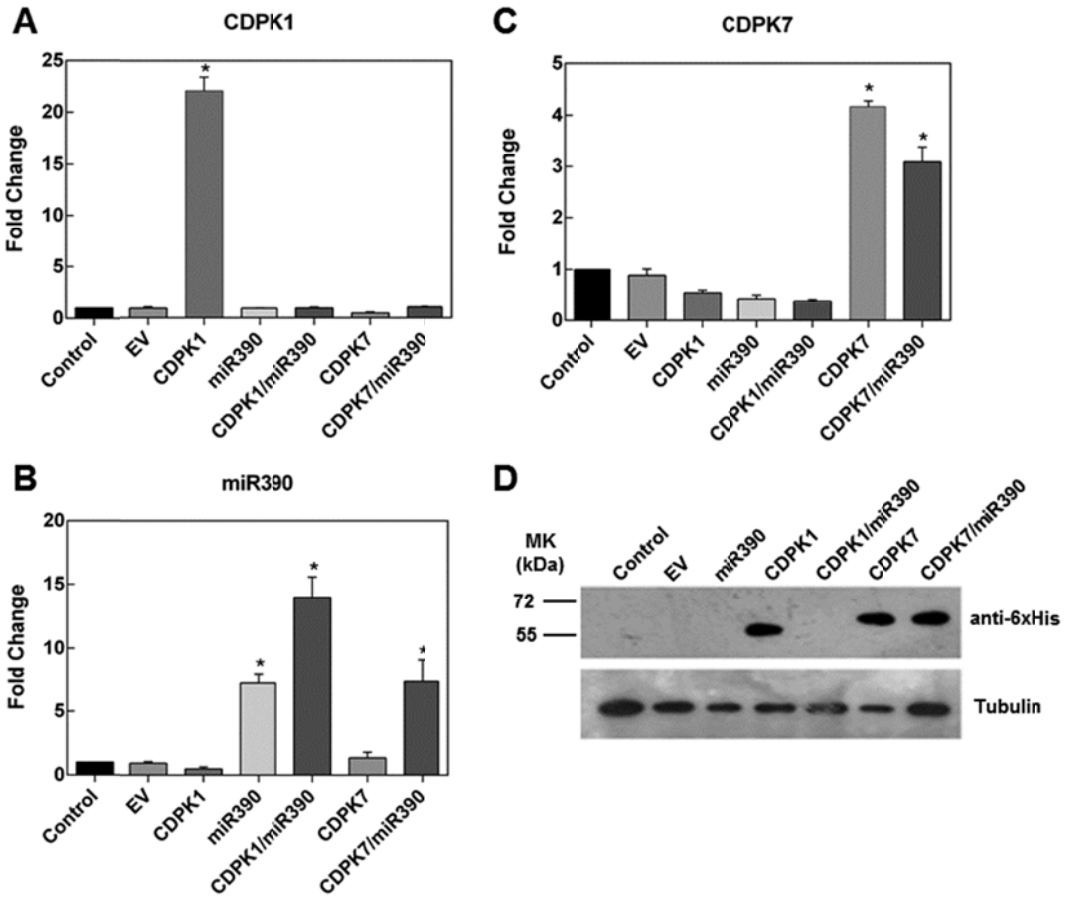

Fig. 5. miR390 targets CDPK1 posttranscriptionally. qRT-PCR expression analysis of (A) StCDPK1, (B) mature miR390 and (C) StCDPK7 in agroinfiltrated *N. benthamiana* leaves and controls (uninfiltrated leaves). EV: Empty vector pGWB408; CDPK1: 35S::CDPK1 + EV; miR390: 35S::miR390precursor + EV; CDPK7: 35S::CDPK7 + EV; CDPK1/miR390: 35S::CDPK1 + 35S::miR390precursor + EV; CDPK7/miR390: 35S::CDPK7 + mi35S::miR390precursor + EV. GAPDH was used for normalization. Means ± SD of three biological replicates each with three technical replicates are plotted. Data were analyzed with One-way ANOVA and Tukey's multiple comparison test (P<0.05). (D) Western blot analysis of protein extracts (50 µg) from agroinfiltrated leaves was performed using anti-polyhistidine antibody (1:7000). Tubulin was used as loading control.

This article is protected by copyright. All rights reserved.

Accepted Article

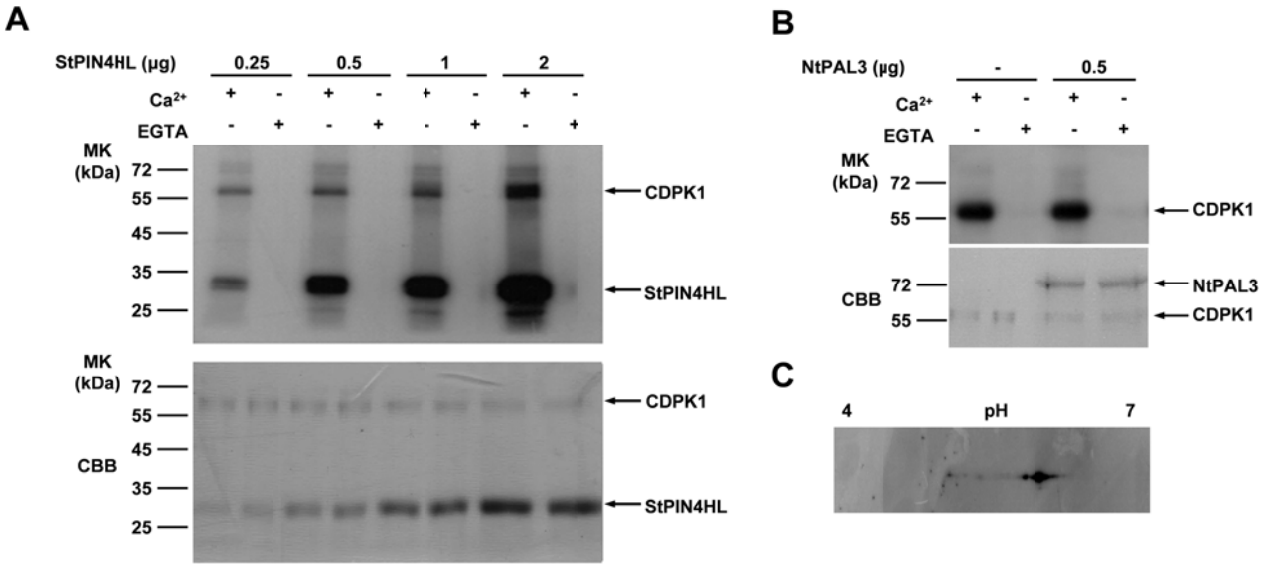

Fig. 6. StPIN4 phosphorylation by CDPK1. (A) Upper panel: Calcium-dependent phosphorylation of increasing amounts of StPIN4 by a constant amount (100 ng) of StCDPK1 Lower panel: Coomassie Brilliant Blue-stained gel. (B) Upper panel: Calcium-dependent StCDPK1 autophosphorylation in the presence or absence of NtPAL3-6xHis. Lower panel: Coomassie Brilliant Blue-stained gel. Phosphorylation assays were performed in the presence of 25 µ*M* calcium or 1 m*M* EGTA. (C) 2D Western blot of autophosphorylated StCDPK1 developed with the anti-polyhistidine antibody (1:5000).

This article is protected by copyright. All rights reserved.

Accepted Article

Table 1. *Cis*-elements predicted in StCDPK1 promoter that could be involved in tissue specification or in hormone regulation of StCDPK1 expression.

[a]Elements also present in *StmiR390* precursor promoter are indicated in bold letters and the number of sites of those elements in *StmiR390* precursor promoter are in brackets. Motif occurrences with a *P*-value<0.0001 were computed using FIMO tool from MEME Suite.

Associated to	*cis*-element	Sequence	Number of sites[a]	*P*-value	Database
Root expression	SP8BFIBSP8AIB	ACTGTGTA	1	1.79E-05	PLACE
	SP8BFIBSP8BIB	**TACTATT**	1 (1)	9.66E-05	PLACE
Storage proteins	**SEF1MOTIF**	**ATATTTAWW**	3 (5)	2.66E-05	PLACE
Xylem expression	AC-I	(T/C)C(T/C)(C/T)ACC(T/C)ACC	1	9.88E-06	PlantCare
	AC-II	(C/T)T(T/C)(C/T)(A/C)(A/C)C (A/C)A(A/C)C(C/A) (C/A)C	1	1.72E-05	PlantCare
Gibberellins	GARE-motif	TCTGTTG	1	6.51E-05	PlantCare
	P-box	**CCTTTTG**	1 (1)	6.51E-05	PlantCare
ABA	**ATHB6COREAT**	**CAATTATTA**	1	7.28E-06	PLACE
Light	**ATC-motif**	**AGTAATCT**	1	2.18E-05	PlantCare
	ATCT-motif	**AATCTAATCT**	4 (1)	1.64E-06	PlantCare
	GAG-motif	**AGAGAGT**	1	6.51E-05	PlantCare
	MRE	**AACCTAA**	1	7.93E-05	PlantCare

This article is protected by copyright. All rights reserved.